ISSN 1011-372X, Volume 137, Combined 1-2

Catal Lett (2010) 137:35–44
DOI 10.1007/s10562-010-0336-x

Resistance to Sulfur and Oxygenated Compounds of Supported Pd, Pt, Rh, Ru Catalysts

J. M. Badano · M. Quiroga · C. Betti · C. Vera · S. Canavese · F. Coloma-Pascual

Received: 9 December 2009 / Accepted: 29 March 2010 / Published online: 13 April 2010

Abstract The poisoning resistance to sulfided and oxygenated compounds of some VIII Group PYGAS selective hydrogenation catalysts based on metals was assessed. Low content alumina supported Rh, Pd, Ru and Pt catalysts (0.35 wt%) were prepared from chlorided precursors. In the case of the palladium catalysts a nitrogenated precursor was also used. The catalysts were mainly assessed in the catalytic test of selective styrene hydrogenation in the presence or absence of known poisons. Model feedstocks spiked with thiophene, thiophane and tetrahydrofuran were used. The catalysts were further characterized by means of chemical analysis, XPS, TPR and chemisorption. The results indicate that chlorided precursors yield more sulfur resistant catalysts. The effect was attributed in part to the formation of oxychlorinated species, refractory to reduction, that leave the metal in an electron deficient state, thus inhibiting the formation of strong poison-metal bonds, the chloride species could also be a steric factor that can contribute to the sulfur resistance of the catalyst. Pd based catalyts had the highest activity and resistance to poisons of all the metals tested. This superior performance was attributed in part to the total occupancy of the 4*d* electronic levels of the Pd metal that was supposed to promote the rupture of the H_2 bond during the hydrogenation reaction.

Keywords Low metal loading catalysts · Selective hydrogenation · Sulfided and oxygenated poisons

J. M. Badano (✉) · M. Quiroga · C. Betti · C. Vera · S. Canavese
INCAPE, Instituto de Investigaciones en Catálisis y Petroquímica, Santiago del Estero 2654, S3000AOJ Santa Fe, Argentina
e-mail: jbadano@fiqus.unl.edu.ar

M. Quiroga
e-mail: mquiroga@fiq.unl.edu.ar

C. Betti
e-mail: cbetti@fiq.unl.edu.ar

C. Vera
e-mail: cvera@fiq.unl.edu.ar

S. Canavese
e-mail: canavese@fiq.unl.edu.ar

M. Quiroga · C. Vera · S. Canavese
Facultad de Ingeniería Química (UNL), Santiago del Estero 2829, S3000AOJ Santa Fe, Argentina

F. Coloma-Pascual
Servicios Técnicos de Investigación, Facultad de Ciencias, Universidad de Alicante, Apartado 99, 03080 Alicante, Spain
e-mail: f.coloma@ua.es

List of Symbols

PF	Poison free condition
TE	Thiophene
TA	Thiophane
THF	Tetrahydrofuran
D	Metal dispersion
S	Metal specific surface ($m^2\ g_{met}^{-1}$)
d	Average metal particle size (Å)
$V_{HAds}^{(CNPT)}$	Volume of hydrogen chemisorbed at normal conditions (cm^3)
PA	Atomic weight of the metal ($g\ mol^{-1}$)
w	Metal content per unit gram of catalyst
M	Mass of sample (g)
v	Stoichiometry of chemisorption of the gas on the surface metal atoms
V_m^{CNPT}	Volume of the chemisorbed monolayer of the adsorbate at normal conditions ($cm^3\ g^{-1}$)
N	Avogadro's number (6.023×10^{23})

V_N	Molar volume of the adsorbate at normal conditions
σ	Number of metal atoms per square meter (atoms m^{-2})
x	Adsorption stoichiometry (number of hydrogen atoms adsorbed per unit of metal atom)
ρ	Density of the metal (g m^{-3})
M_{Red}/M_{Tot}	Reduced metal amount and total metal amount ratio
wt M%	Nobel metal content (weight percentage)
T_{Red}	Reduction temperature (K)
r°_{ES}	Initial styrene hydrogenation rate in poison free condition (mol g_{cat}^{-1} min^{-1})
DES	Relative deactivation per concentration of poison (ppm^{-1})

1 Introduction

Selective hydrogenation catalytic reactions are of vital importance in the petrochemical and petroleum refining industries. For example 35% of the gasoline consumed in the last decade in the USA came from cracking processes. Moreover, the latter have supplied ca. 20–40% of the gasoline consumed in the whole world [1, 2]. Pyrolisis gasolines (PYGAS) are a light boiling range subproduct of the high temperature pyrolysis processes [3]. Usually PYGAS streams comprise cuts of carbon length C_5–C_{12}. Due to the high content of aromatics and olefins pyrolysis gasolines are used as high octane compounds for blending in the gasoline pool or as a highly unsaturated feedstock for aromatic extraction. Up to 15% of PYGAS compounds are highly reactive mono and diolefins' and tend to form gums in vessels, pipelines and catalysts and must be eliminated from the feedstock of most refinery units [1].

The industrial process used to stabilize the PYGAS stream is a two-step catalytic selective hydrogenation [4]. In the first step olefins, diolefins and styrene are hydrogenated using alumina supported Pd or Ni catalysts at moderate pressure and temperature conditions [5]. The second stage has the objective of removing sulfur compounds and remaining olefins. Catalysts for this stage are alumina supported cobalt–molybdenum catalysts. These are operated at more severe conditions than catalysts of the first stage [4].

The main problem of catalysts for the removal of reactive olefins is that PYGAS streams contain a high content of sulfur, usually between 300 and 2000 ppm [1, 2]. Thiophenes are the main sulfur compounds causing catalyst deactivation.

Styrene hydrogenation over Pd and Ni catalysts at moderate reaction conditions has been particularly studied [1, 5]. It is considered a laboratory model reaction for assessing the performance of PYGAS purification catalysts because it is one of the most refractory compounds of these streams [1]. It is also used in the industrial practice as a test reaction for assessing the performance of the hydrogenation catalysts under real conditions [6].

In one of our previous works [7] we evaluated the activity of many alumina supported metal catalysts and found that Pd catalysts were the most active in the selective hydrogenation of styrene to ethylbenzene. In this work our attention is focussed on the resistance of these metal catalysts, namely Ru, Rh, Pd and Pt, to the poisoning by oxygen and sulfur compounds. Thiophene and thiophane are used as model sulfided poisons while tetrahydrofurane is used as a model oxygenated poison.

2 Experimental

2.1 Catalysts Preparation

The catalysts were prepared by incipient wetness technique using CK-300 γ-Al_2O_3 as support (ground and sieved to 35–80 meshes, calcined at 823 K during 4 h, 180 m^2 g^{-1} BET surface area). To study the influence of the metals and of the precursor salts, different acidic solutions were prepared. The precursors employed were: $PdCl_2$ and $Pd(NO_3)_2{\cdot}2H_2O$ (Fluka, purity >99.98%), $RuCl_3{\cdot}H_2O$, $RhCl_3{\cdot}xH_2O$ and $H_2PtCl_6{\cdot}H_2O$ (Strem Chemicals, purity >99.9%). Different acidic solutions of the chloride precursor salts were prepared using HCl at pH = 1. For $Pd(NO_3)_2{\cdot}2H_2O$ an acidic solution was prepared using HNO_3 at pH = 1. The concentration of the solutions was calculated in order to obtain a metal loading, M/γ-Al_2O_3 (with M = Pd, Ru, Pt, Rh), of 0.35 wt%. The impregnated solids were dried during 24 h at 393 K, and then they were calcined under an air flow during 4 h at different temperatures: Pd at 673 K and Pt, Ru and Rh at 773 K. Prior to reaction, the catalysts were reduced in flowing hydrogen during 1 h at different temperatures: Pt, Ru and Rh at 673 K, Pd prepared from $PdCl_2$ at 373 and 673 K, and Pd prepared from $Pd(NO_3)_2$ at 423 K. These reduction temperatures were selected after inspection of the TPR traces. The temperatures values should be sufficiently high so as to guarantee total reduction of the metal and sufficiently low to avoid sintering of the metal phase. For the most active and poison resistant catalyst, the influence of the precursor salt and of the reduction temperature was studied.

2.2 Chemical Analysis

The metal loading of the catalysts was obtained by spectrophotometric determinations.

2.3 Temperature Programmed Reduction

The tests were performed in a Micromeritics Auto Chem II apparatus equipped with a thermal conductivity detector. A cold water trap was placed before the thermal detector to condense water. Before the TPR tests the samples were dried in situ at 423 K for 1 h under an argon flow (AGA purity 99.99%). After that the samples were cooled up to 250 K in the same atmosphere. Then the temperature was increased up to 800 K at 10 K min^{-1} in a gas flow (5% (v/v) hydrogen in argon) at a total flow rate of 40 mL min^{-1}.

2.4 Pulse Chemisorption

Hydrogen chemisorption was performed and dispersion values were obtained after reducing each sample at the above mentioned temperatures using a Micromeritics Auto Chem II apparatus equipped with a thermal conductivity detector. The samples were degassed in situ for 2 h under an argon flow (AGA, 99.99%) at a temperature equal to that of the corresponding reduction step and then cooled at room temperature except palladium catalysts, which were cooled at 373 K where the formation of palladium hydride is negligible [8]. After that, the chemisorption of hydrogen was performed.

The hydrogen chemisorption technique apart from enabling the calculation of the metal dispersion (D) it also gives an estimate of the specific surface area (S) and the average particle size of the alumina supported metal particles (d). Dispersion was calculated by means of Eq. 1, using the total amount of metal and regardless of its degree of reduction. Metal specific surfaces areas were calculated using the equation of Paryjczac and Szymura [9] (see Eq. 2). The metal particle size was determined on the basis of a spherical particle. Such an election is mainly backed by the results reported by Paryjczak and Szymura [9] who performed an extense study using electronic microscopy and found that this model better correlated the microscopy results with those obtained by chemisorption. Equation 3 depicts this model.

$$D(\%) = \frac{v \cdot V_{\mathrm{HAds}}^{(\mathrm{CNPT})} \cdot \mathrm{PA}}{22414 \cdot w \cdot M} \times 10^5 \quad (1)$$

$$S = \frac{2 \cdot N \cdot V_{\mathrm{m}}^{\mathrm{CNPT}}}{w \cdot V_{\mathrm{N}} \cdot \sigma \cdot x} \quad (2)$$

$$d = \frac{6 \cdot \sigma \cdot \mathrm{PA}}{\rho \cdot N \cdot D} \quad (3)$$

In these equations $V_{\mathrm{HAds}}^{(\mathrm{CNPT})}$ is the volume of hydrogen chemisorbed at normal conditions of pressure and temperature (cm^3); PA the atomic weight of the metal (g mol^{-1}); w the metal content per unit gram of catalyst; M the mass of the sample used in the test (g); and v the stoichiometry of chemisorption of the gas on the surface metal atoms. All the metals used in this work are known to dissociatively chemisorb hydrogen. For this reason the used chemisorption stoichiometry was $v = 2$ metal atoms per hydrogen molecule, i.e. H/M = 1 [10]. S is the specific surface area of the metal (m^2 g^{-1}); $V_{\mathrm{m}}^{\mathrm{CNPT}}$ is the volume of the chemisorbed monolayer of the adsorbate at normal pressure and temperature (cm^3 g^{-1}); N is Avogadro's number (6.023×10^{23}); V_{N} is the molar volume of the adsorbate at normal conditions of pressure and temperature; σ is the number of metal atoms per square meter; x is the adsorption stoichiometry (number of hydrogen atoms adsorbed per unit of metal atom); d is the average diameter of the metal particles (Å) and ρ is the density of the metal (g m^{-3}). The adopted σ value was calculated from the average of the densities of the (100), (110) and (111) crystal planes [11, 12].

2.5 X-Ray Photoelectron Spectroscopy (XPS)

The superficial electronic state of each metal and of chlorine and their atomic ratios were studied by X-ray Photoelectron Spectroscopy (XPS) following the Pd $3d_{5/2}$, Pt $4d_{5/2}$, Rh $3d_{5/2}$, Ru $3d_{5/2}$.and Cl $2p_{3/2}$ peaks position, respectively. As a consequence of the interference of the Al 2p line, the Pt $4d_{5/2}$ peak position was followed instead of the most common Pt $4f_{7/2}$. To correct possible deviations caused by electronic charge on the samples, the Al 2p line was taken as an internal standard at 74.4 eV. Measurements were made using a VG-Microtech Multilab equipment, a Mg Kα ($h\nu$: 1253.6 eV) radiation and a pass energy of 50 eV. The XPS system analysis pressure was kept at 5×10^{-7} Pa. Samples were treated in situ with H_2 following the same procedure as that for catalyst preparation. A careful deconvolution of the spectra was made. The areas under the peaks were estimated by calculating the integral of each peak after subtracting a Shirley background and fitting the experimental peak to a combination of Lorentzian/Gaussian lines of 30–70% proportions [13].

2.6 Catalytic Reaction Tests

Styrene hydrogenation was carried out in a batch PTFE coated stainless steel stirred tank reactor. In each poison-free test the reactor was loaded with 200 mL of a solution of 10% (v/v) styrene (Aldrich, Cat. N° S497-2, purity >99%) in toluene (Merck, Cat. N° TX0735-44, purity >99%),

using *n*-decane (Fluka, Cat. N° 30550, purity >98%) as an internal standard. The reactor was maintained at 353 K and a constant H_2 pressure of 10 bar while being stirred at 800 rpm. Runs were carried out in triplicates with an average experimental error of 3%, using 0.2 g of catalyst and a styrene/metal molar ratio equal to 2.6×10^4. In the case of the catalytic tests in the presence of poisons concentration values of 300 ppm of thiophene, 50 ppm of thiophane or tetrahydrofuran were used, at identical operational conditions. The solutions were prepared by dropwise addition of the poison to the original solution with a calibrated syringe.

Internal and external diffusional limitations were absent in the conditions of this work. Reactant and products were analyzed by gas chromatography using a Shimadzu GC-2010 equipped with a FID detector and a 30 m J&W INNOWax 19091N-213 (cross-linked polyethylene glycol phase) capillary column.

3 Results and Discussion

Figure 1 shows the TPR trace of the γ-Al_2O_3 support calcined at 773 K. A negative peak at 773 K indicates that water is evolved as a consequence of the thermal decomposition of the gamma phase and the sintering of the material [14]. 773 K was hence chosen as the upper limit for the calcination of the prepared catalysts. The presence of the gamma phase of the support was confirmed by inspection of the corresponding XRD spectrum.

Figure 1 also contains the TPR trace of RhCl. This has a broad reduction peak at 370–700 K. The reason of this wide peak can be due to the strong interaction of the Rh oxides with the support. Different authors have reported that this effect is enhanced upon increasing the temperature of calcination of the catalyst [15, 16]. The interaction between the Rh oxides and the support would be due to the migration of oxide species inside the uppermost surface layer of the alumina during the heat treatments, specially at temperatures higher than 773 K [15, 16]. On the base of our TPR results and the literature reports the wide peak should be related to the reduction of Rh_2O_3 oxide species with different degrees of interaction with the support [15–18].

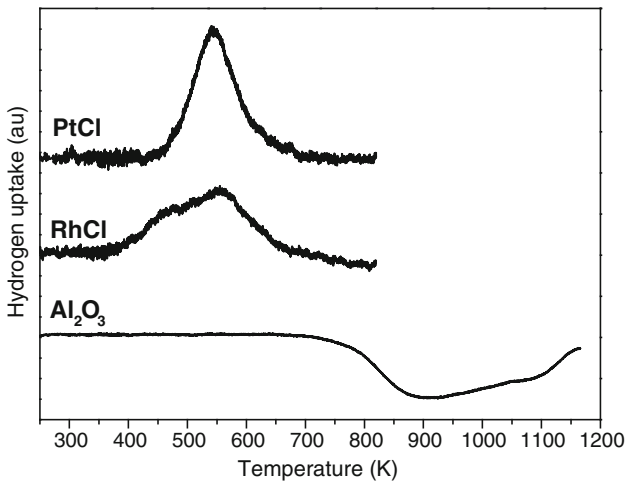

Fig. 1 TPR traces of the Al_2O_3, RhCl and PtCl catalysts

Figure 1 also shows the reduction trace of the PtCl catalyst. This has a wide peak spanning the 430–700 K range. Lieske et al. [19] have reported that Pt/Al_2O_3 catalysts prepared from chlorinated precursors have two peaks in their TPR trace that are due to complex surface species containing chlorine. One peak at 533 K was attributed to $[Pt^{IV}(OH)_xCl_y]$ while another at 563 K was attributed to $[Pt^{IV}O_xCl_y]$. The formation of these species depends on the temperature of calcination of the catalyst [20]. Reyes et al. [21] have attributed the peak at 420–460 K to the reduction of PtO_2 and the peak at about 600 K to the reduction of PtO_xCl_y. Finally Navarro et al. [22] have reported that silica–alumina supported Pt catalysts prepared from H_2PtCl_6 display a broad reduction peak at 300–700 K and they suggest that this broad envelope contains many merged peaks of oxygen and chlorine containing species such as $Pt(OH)_xCl_y$, PtO_xCl_y and PtO_2. In accordance to this bibliography and the calcinations temperature used (773 K) the wide peak observed in Fig. 1 between 430 and 700 K of the platinum catalyst should be related to the reduction of $Pt^{\delta+}O_xCl_y$ oxychlorinated species.

Figure 2 contains the TPR traces of the PdN and PdCl catalysts. Both catalysts have a reduction peak at 291 K that can be assigned to the presence of bulk PdO particles that are easily reduced. These particles are agglomerated over the support during the calcination of the catalyst as it has been extensively reported in the related literature [22–24]. Figure 2 also shows that the PdN and PdCl samples have a negative peak at about 335 K that is supposedly due to the issue of H_2 during the decomposition of the β phase of palladium hydrides (β-HPd) that is formed during the reduction of the PdO particles at low temperatures [10, 22–25]. The PdCl catalyst also has a broad reduction peak at 400–500 K that is not present in the TPR trace of the PdN sample. Some authors attribute this peak to the reduction of PdO species strongly interacting with the support [5, 24, 26]. Other authors suggest that the hydrogen consumption at these temperatures is due to the reduction of $Pd_xO_yCl_z$ oxychlorinated species or the reduction of Pd^{2+} ions stabilized by adjacent Cl^- remaining after the calcination process [27–29]. The difference in reduction pattern depending on the kind of metal precursor and on whether this precursor is chlorinated or not has been pointed out by many authors studying the Pt catalysts. In the case of

supports impregnated with chlorinated Pt precursors their calcination produces surface $Pt^{IV}O_xCl_y$ species, non-chlorinated precursors produce PtO_2 species [20].

Figure 2 also contains the TPR trace of the RuCl catalyst. A peak at 370 K can be seen and it is attributed to easily reducible RuO particles [30]. Many authors have reported that above 523 K Ru is in a completely reduced state [30, 31].

The temperature of reduction of the catalysts were chosen after inspection of the TPR traces. Temperatures that ensured total reduction were seeked but these had to be as low as possible to inhibit sintering. 423 K was adopted for the Pd catalysts prepared from $Pd(NO_3)_2$ and 673 K for the Pt, Rh and Ru catalysts. In the case of the Pd catalyst prepared from the chloride salt two reduction temperatures were adopted (373 and 673 K) in order to study the influence of these temperatures on the activity, selectivity and poison resistance.

Table 1 shows results of the degree of reduction of the different catalysts (M_{Red}/M_{Tot}, reduced metal amount and total metal amount ratio). These values were obtained by integration of the TPR trace. The calculations were performed using the following stoichiometry of reduction: $H_2/Pd^{2+} = 1, H_2/Pt^{4+} = 2, H_2/Rh^{3+} = 3/2$ and $H_2/Ru^{+2} = 1$.

The results of M_{Red}/M_{Tot} in Table 1 indicate that in the case of the PdN catalyst Pd is completely reduced while in the case of the PdCl catalyst Pd is reduced only 16 or 31% depending on the reduction temperature employed. The higher temperature the higher amount of reduced metal. This difference in the percentages of reduction could be possibly due to the formation of Pd oxychloride species of difficult reducibility formed during the calcination treatment.

Similarly to Pd, Pt is not completely reduced and this is possibly due to the presence of refractory Pt oxychlorinated species. The metal in the Rh catalyst is reduced to a 70%. This could be due to the migration of rhodium oxide species to subsurface layers of the alumina support. Such phenomenon occurs during the calcination treatment and makes total reduction of Rh difficult [15, 16]. Ru was practically completely reduced to the metallic state.

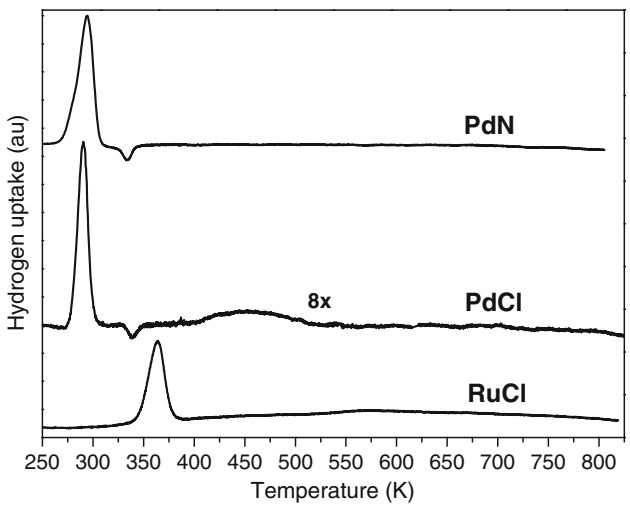

Fig. 2 TPR traces of the RuCl, PdN and PdCl catalysts

3.1 Metal Dispersion Results

The metal dispersion (D) results are listed in Table 1 along with the values of metal specific surface (S) and average metal particle size (d), as determined by the hydrogen chemisorption technique. Table 2 shows the values of σ and ρ of the metals used in Eqs. 2 and 3.

From Table 1 it can be seen that Pd and Pt catalysts have the lowest particle sizes (between 3 and 4 nm). Also, it can be seen that the PtCl and PdCl samples show the highest dispersion values. The lower particle size and the higher dispersion of the Pd catalysts prepared from chlorinated precursors can be due to the presence of complex oxychlorinated species formed during the calcination process. The presence of these species improves the metal dispersion due to the greater interaction between these oxychlorinated species and the support as compared to the weaker one displayed by Pd oxide (PdO) [5, 32–34]. The alumina supported Pt catalysts have a higher metal dispersion as compared to the other metal catalysts. This higher dispersion is attributed to the strong interaction between Pt oxychlorinated species ($Pt^{\delta+}O_xCl_y$) and the alumina surface groups. This interaction is the highest among the metals studied and would appear upon the calcination of the catalyst at temperatures higher than 773 K [20].

The alumina supported Ru catalyst displayed dispersion values (D) lower than 5%. An accordingly high value of metal particle diameter (d) was obtained by means of Eq. 3. Similar values of D and d have been reported for ruthenium metal catalysts that undergo the same series of treatments employed in this work [16, 35, 36]. The high degree of sintering of the Ru metal particles could be due to the fact that no oxychlorinated species interacting with the alumina support are formed during the calcination process, as earlier noted by Lederhos et al. [13] while studying ruthenium catalysts of high metal content.

3.2 XPS Results

Figure 3 shows the XPS spectra of the palladium: PdN423 (a), PdCl673 (b) and PdCl373(c), platinum PtCl673 (d), rhodium RhCl673 (e) and ruthenium RuCl673 (f) catalysts. The metals binding energies (BE M) and Cl/M atomic ratios are also listed in Table 1. As shown in Fig. 3a, the Pd $3d_{5/2}$ peak of PdN423 catalyst had a peak with a value of

Table 1 Catalyst properties

Property	Catalysts					
	PdCl673	PdCl373	PdN423	PtCl673	RhCl673	RuCl673
wt $M\%$[a]	0.34	0.34	0.31	0.33	0.32	0.30
T_{Red} (K)[b]	673	373	423	673	673	673
M_{Red}/M_{Tot} (%)[c]	31	16	99	78	70	97
D (%)[d]	38	37	26	39	20	3
S (m^2 g_{met}^{-1})[e]	169	157	107	99	102	12
d (Å)[f]	29	30	43	29	55	445
BE M (eV)[g]	335.4	335.9	334.7	313.8[1] 315.8[2]	306.9	279.5
Cl/M (at at^{-1})[h]	1.6	10.9	0	2.4	0	0
r°_{ES} (mol g_{cat}^{-1} min^{-1})[i]	0.0327	0.0281	0.0261	0.0121	0.0100	0.0012
DES°_{TE} (ppm_{TE}^{-1})[j]	0.204	0.197	0.227	0.229	0.307	–
DES°_{TA} (ppm_{TA}^{-1})[k]	1.174	1.074	1.402	1.554	1.860	–
DES°_{THF} (ppm_{THF}^{-1})[l]	0.256	0.364	0.214	1.530	1.206	–

[a] Nobel metal content, weight percentage

[b] Reduction temperature

[c] Percentage of metal reduction

[d] Dispersion of the metal

[e] Specific surface area of the metal

[f] Average radius of the metal particle

[g] Pd $3d_{5/2}$, Pt $4d_{5/2}$, Rh $3d_{5/2}$ or Ru $3d_{5/2}$ binding energies

[h] Chlorine/metal ratio

[i] Initial styrene hydrogenation rate (PF)

[j,k,l] Relative deactivation per initial concentration of poison $DES = ((1 - r^{\circ}_X/r^{\circ}_{ES})/C^{\circ}_X) \times 100$

[1] 28% at/at

[2] 72% at/at

Table 2 Bulk molar and atomic surface density values [11, 12]

Metal	Molar density, ρ (mol m^{-3})	Surface atomic density, σ (atoms m^{-2})
Palladium	1.202×10^7	1.27×10^{19}
Platinum	2.145×10^7	1.25×10^{19}
Rhodium	1.240×10^7	1.33×10^{19}
Ruthenium	1.230×10^7	1.63×10^{19}

binding energy of 334.7 eV that corresponds to Pd^0 [37] while the PdCl673 and PdCl373 catalysts (Fig. 3b, c) displayed peak values of 335.4 and 335.9 eV, respectively. These higher binding energy values indicate that the metal is electrodeficient ($Pd^{\delta+}$) possibly due to the presence of non-reduced Pd oxychloride species formed during the calcination process [33] or due to the presence of non-reduced Pd species stabilized by neighbour Cl atoms [5, 38, 39]. The low reduction temperature employed generated a more electrodeficient Pd with high Cl superficial content.

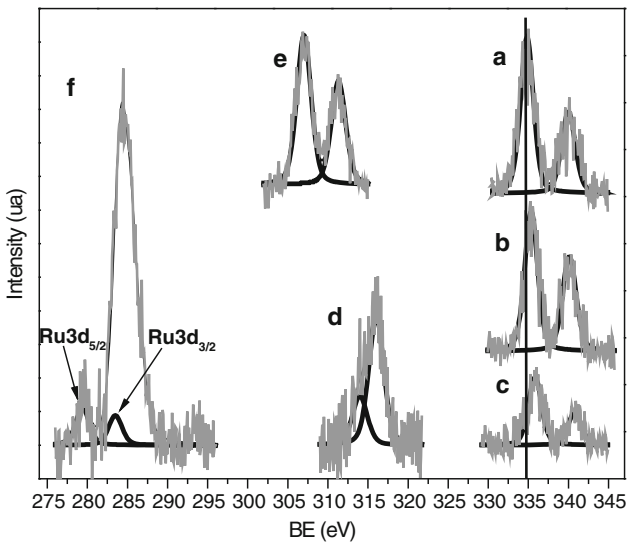

Fig. 3 XPS spectra of the palladium: PdN423 (**a**), PdCl673 (**b**) and PdCl373 (**c**), platinum PtCl673 (**d**), rhodium RhCl673 (**e**) and ruthenium RuCl673 (**f**) catalysts

In the case of the PtCl673 sample after the deconvolution of the Pt $4d_{5/2}$ spectra two signals can be seen (Fig. 3d) at 313.8 (28% of all metal species, atomic basis) and 315.8 eV (72% at/at) that can be attributed to Pt^0 (28% at/at) and $Pt^{(\delta+)}$ complex species (72% at/at) stabilized by Cl^- that are formed during the calcination treatment. According to the bibliography the electrodeficiency of Pd and Pt ($\delta+$) is between 0 and 2 [37]. The XPS spectra of the Pd and Pt catalysts prepared from chlorine precursors (PdCl673, PdCl373 and PtCl673) show a peak at ca. 198.5 eV that corresponds to Cl $2p_{3/2}$. The peak was associated to surface chloride species [37] that were not complete eliminated after reduction.

Finally in the case of the RhCl673 sample (Fig. 3e) a $3d_{5/2}$ peaks binding energy value a signal was obtained at 306.9 eV. The Ru 3d XPS peak was carefully deconvoluted (Fig. 3f), the Ru $3d_{3/2}$ peak appears superposed to the C 1s line, for a sake of clarity the C 1s deconvolution lines are not shown in Fig. 3f to make more clear the presentation. For the RuCl673 sample a $3d_{5/2}$ peaks binding energy value a signal was obtained at 279.5 eV. The BE values found for the Rh and Ru samples correspond to the completely reduced metallic state [37].

In Table 3 are summarized the XPS and TPR characterization of the studied catalysts with the external *d* orbital for the characterized metal species.

3.3 Catalytic Activity Results

According to the internal standard method the selectivity for all the catalysts during the different evaluations was ca. 98%. No hydrogenolysis of the poisons was detected. Figures 4, 5, 6 and 7 show the results of conversion as a function of time obtained in the catalytic test runs performed without the presence of poisons and with the presence of tiophene, tiophane and tetrahydrofurane, respectively. In all the systems tested, the initial reaction order of styrene was 0 and changed to 1 at high conversion values. Therefore a Langmuir–Hinshelwood-type kinetic model can be suggested [7].

Table 1 contains the initial activity results corresponding to the runs without poison (r°_{ES}) and the values of relative deactivation of the catalysts due to different poisons (DES). This deactivation is calculated as $DES = ((1 - r^\circ_X/r^\circ_{ES})/C^\circ_X) \times 100$ where r°_X is the initial

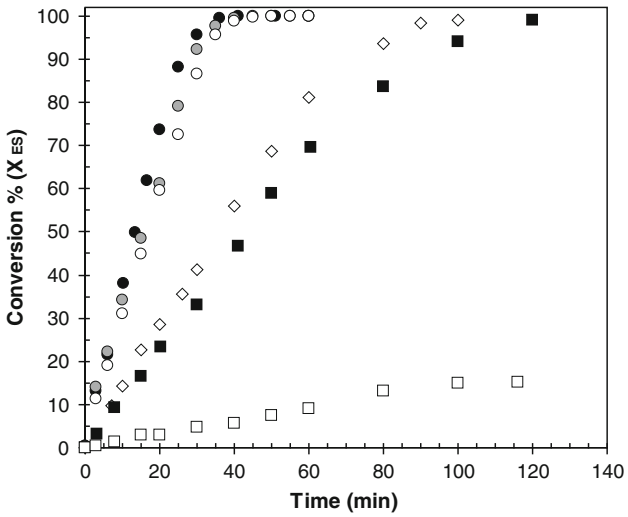

Fig. 4 Styrene conversion as a function of time in the absence of poisons. (●) PdCl673, (●) PdCl373, (○) PdN423, (◇) PtCl673, (■) RhCl673, (□) RuCl673

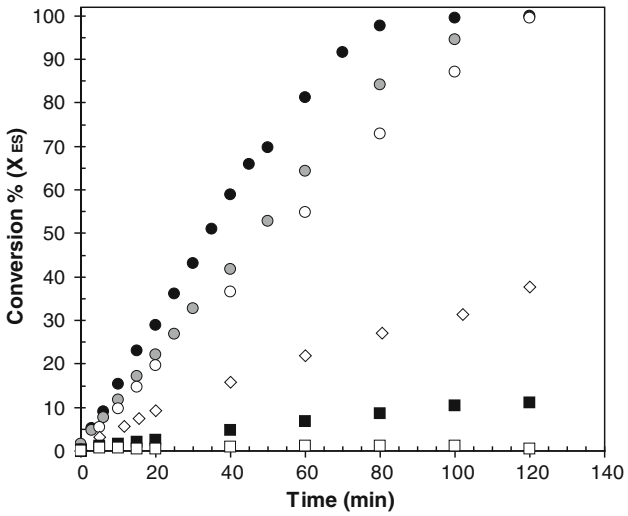

Fig. 5 Styrene conversion as a function of time in the presence of thiophene. (●) PdCl673, (●) PdCl373, (○) PdN423, (◇) PtCl673, (■) RhCl673, (□) RuCl673

Table 3 XPS and TPR characterization of the catalysts and external *d* orbital for the characterized metal species

Catalyst	Metal oxidation state	Possible metal species	Metal external *d* orbital
PdN423	Pd^0	Pd^0	$4d^{10}$
PdCl673	$Pd^{\delta+}$ ($\delta < 2$)	$Pd_xO_yCl_z$	$4d^n$ ($8 \ll n < 10$)
PdCl373	$Pd^{\eta+}$ ($\delta < \eta < 2$)	$Pd_xO_yCl_z$	$4d^m$ ($8 < m < n < 10$)
PtCl673	Pt^0 (28%)	Pt^0 (28%)	$5d^9$
	$Pt^{\delta+}$ (72%, $\delta < 2$)	$Pt^{\delta+}O_xCl_y$ (72%)	$5d^n$ ($8 < n < 9$)
RhCl673	Rh^0	Rh^0	$4d^8$
RuCl673	Ru^0	Ru^0	$4d^7$

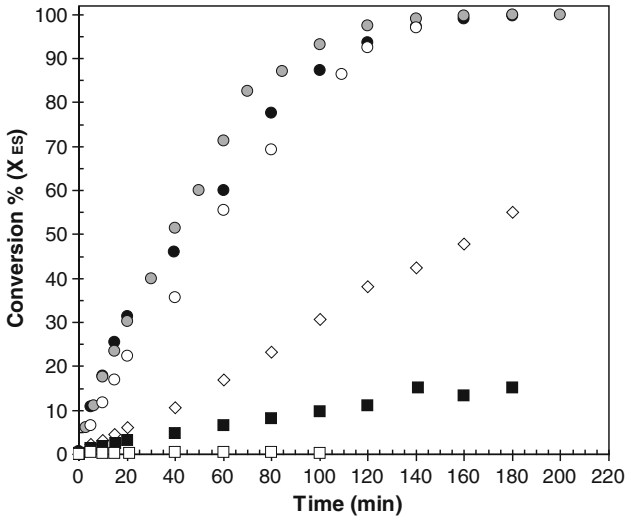

Fig. 6 Styrene conversion as a function of time in the presence of thiophane. (●) PdCl673, (●) PdCl373, (○) PdN423, (◇) PtCl673, (■) RhCl673, (□) RuCl673

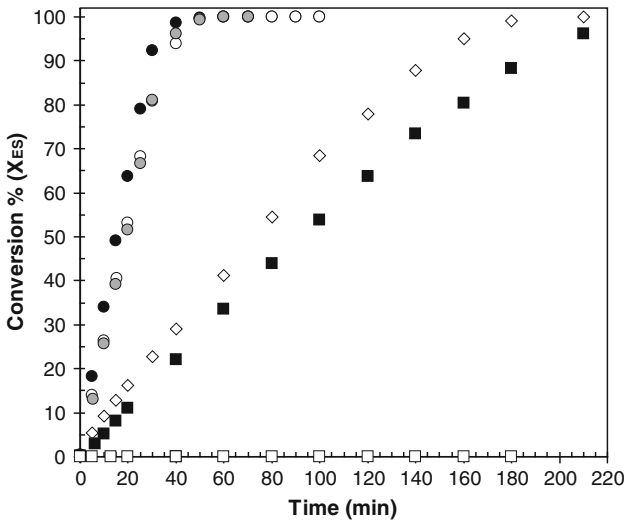

Fig. 7 Syrene conversion as a function of time in the presence of tetrahydrofuran. (●) PdCl673, (●) PdCl373, (○) PdN423, (◇) PtCl673, (■) RhCl673, (□) RuCl673

activity recorded in the test with the feedstock spiked with tiophene (X = TE), tiophane (X = TA) and tetrahydrofurane (X = THF), and $C°_X$ is the initial concentration of poison.

The results of Fig. 4 and Table 1 indicate that in the case of the systems with no poison Pd catalysts are the most active catalysts for styrene conversion. They reach 100% conversion in about 45 min. For the most active catalyst the effect of the precursor salt and the reduction temperature was evaluated. In this case the activity values recorded for the palladium system slightly varies depending on the metal precursor or the reduction temperature used.

The inspection of the results of Figs. 5, 6 and 7 shows that the order of resistance to poisoning was: Pd > Pt > Rh ≫ Ru. In the poisoned palladium systems total conversion of styrene was achieved at 45 or 160 min for a poisoning level of 50 ppm of THF or TA, and 150 min for 300 ppm of TE. The deactivation values showed in Table 1 (DES) indicate that the activity of the Pd catalysts in the presence of poisons depends on the electronic state of the metal. Therefore, the metal precursor and the calcination or reduction temperatures have a crucial role on the performance of the catalyst. It has been thoroughly established in the scientific literature that the poisoning mechanism of Pt and Pd catalysts by sulfur compounds is due to the effect of electron donation from the Group VIII metals to the sulfur atoms [40, 41]. This mechanism could explain the different results obtained with the Pd catalysts. According to the XPS results PdCl373 is more electrodeficient than PdCl673 and in turn this is more electrodeficient than the PdN423 catalyst. The most electrodeficient palladium catalyst is also the most sulfur resistant one. As the most sulfur resistant catalyst has the highest electrodeficient Pd species, this could indicate that the S atom is acting as a Lewis acid center while Pd is acting as a Lewis base. Comparing the deactivation by tiophene with that produced by thiophane we can see that the latter is a stronger poison. One possible explanation is that the S atom of thiophane is directly adsorbed on the metal particles via a σ bond [42] with the metal d electrons (strong η_1-bond). On the other hand thiophene interacts with the metal surface in a planar way through the π electrons of the aromatic nucleus (weaker η_5-bond) [42] and thus displays a smaller metal–poison interaction.

Catalysts containing Pd were the most sulfur-resistant ones. The PdCl373 catalyst was the most resistant catalyst in this series. The high thioresistance of the catalysts synthesized from chlorided salts could be due to the formation of complex oxychlorinated species on the surface that would keep Pd in an electron deficient state. Electron deficiency would inhibit the adsorption of poisons on the metal surface. The Pd catalyst prepared from $Pd(NO_3)_2$ is the least sulfur resistant catalyst probably because in this case the metal is completely reduced under reaction conditions as it was demonstrated by the XPS and TPR tests.

If we analyse the effect produced by the O and S atoms of the THF and TA molecules it becomes evident that there is a marked difference in electronegativity and size, both factors acting in opposite directions. Table 1 results show that THF is a much weaker poison than TA especially in the case of the Pd catalysts. This suggests that the size effect and the Lewis acid strength determine the magnitude of the poisoning. In the case of the TA poison the following

deactivation order can be obtained from Table 1: PdCl373 < PdCl673 < PdN423. In contrast, the totally reduced Pd catalyst is the most resistant to THF poisoning. This effect could be partly due to the fact that oxygen in the THF molecule can only act as electron donor (Lewis base center) in contrast to sulfur that in the TA molecule can expand its octet and act as an electron acceptor (Lewis acid center). So the THF molecule would be directly adsorbed over the metal particles (acid center) via a σ bond between d electrons (η_1-bonded). With respect to the behaviour of the catalysts in the presence of tetrahydrofuran, the Pd catalysts were only slightly affected in comparison to the other supported metal catalysts. The most resistant catalyst to the oxygenated poison was PdN423. This could be due to the fact that Pd^0 has a fully occupied external d orbital and that the O atom in the THF molecule is acting as an electron donor Lewis base.

Compared to the Pt catalyst the Rh catalyst is more resistant to THF. However, Pt in the poisoned state keeps being more active than Rh. The low resistance to THF (a polar poison) of PtCl673 could be due to the presence of surface $Pt^{\delta+}O_xCl_y$ oxychlorinated species with high affinity for polar compounds.

The RuCl673 catalyst is the least active catalyst for hydrogenating styrene and is completely poisoned by sulfided or oxygenated compounds.

It is well known that during reactions of hydrogenation reactions metallic centres rich in electrons can cleave the bonds in H_2 by means of the interaction of a filled d metal orbital with the empty sigma antibonding molecular orbital of H_2 [43]. The rupture of the hydrogen bond is more easily done on metals with a high amount of available electrons in the external d orbital, as it is the case of palladium. This rupture should be less likely on metals with fewer d electrons, as in the case of Ru. Therefore, the differences in activity between the reported catalysts could be partly attributed to differences in the electronic density of the external d orbital of each metal.

During the poisoning tests with TE, TA or THF some electrons of the metal d orbital are shared with S and O atoms. Hence the metals have a smaller amount of available d electrons to promote the hydrogen bond rupture and the catalytic activity is decreased. The worst cases are those involving TE and TA as poisons because the metal acts as an electron donor centre (Lewis base).

On other hand we must consider that surface chloride species present in the PdCl373, PdCl673 and PtCl673 catalysts (detected by XPS, see Table 1) could be responsible for hindering the adsorption of poisons. They have a big size (steric factor) and they are highly electronegative (electronic effect).

Finally if we compare the $Pd_x^{\delta+}O_yCl_z$ and the $Pt^{\delta+}O_xCl_y$ complex species (with $\delta < 2$) we see that in spite of the similar electronic configuration of their external d orbitals some differences can be pointed out: (a) the complexes have different amount of chloride species; (b) the main d level of Pd is different from that of Pt and therefore their HOMO and LUMO frontier orbitals are also different. The HOMO orbital can cleave H–H bonds while the LUMO orbital can receive electron density from the substrate molecule. This means that they can activate styrene for the hydrogenation reaction. From this discussion it can be inferred that both electronic and steric factors exist and that they could explain the differences found in the values of activity and poison resistance of the oxychlorinated complexes of Pd and Pt catalysts.

4 Conclusions

During the selective semi-hydrogenation of styrene, palladium, rhodium, platinum and ruthenium catalysts with low metal loading displayed high selectivity values (ca. 98%). In all catalytic tests, either in absence or presence of poisons, the following order of activity was obtained: Pd > Pt > Rh $\gg$ Ru. It can be rationalized that the hydrogen bond cleavage is more easily performed on the metal with the highest amount of electrons in the external d orbital (Pd) and more difficultly on the metal with the smallest number of d electrons (Ru). The different activity and poison resistance displayed by the catalysts could be partly attributed to a different electronic density in the external d orbital of the metal. In this sense, though Pd and Pt oxychlorinated species have a similar d electron level occupancy, they have very different HOMO and LUMO frontier orbitals responsible for styrene-hydrogen bonding and these energy differences might translate into much different catalytic properties.

The poison tolerance is strongly affected by the kind of precursor salt and the pretreatment employed during the preparation of the Pd catalysts. In the case of the sulfur poisoning tests the metal acts as an electron donor centre. Conversely with oxygenated poisons the metal acts as an electron acceptor center. Thiophene interacts with the metal d electrons in a planar way through the π electrons of the aromatic nucleus (weak bond). Thiophane and tetrahydrofuran are directly adsorbed on the metal particles via a σ bond (strong bond). It can also be possible that chloride complex species present in the surface could hinder the adsorption of poisons via a steric factor (big size of chlorine ligands) or an electronic one (high electronegativity).

Acknowledgements The experimental assistance of C. Mázzaro and the financial assistance of CONICET, ANPCyT and UNL are greatly acknowledged.

References

1. Nijhuis TA, Dautzenberg FM, Moulijn JA (2003) Chem Eng Sci 58:1113
2. Choi JS, Maugé F, Pichon C, Fourcade JO, Jumas JC, Clair CP, Uzio D (2004) Appl Catal A Gen 267:203
3. Gaspar AB, Silva MAP, Araú jo OQF, Medeiros JL, Britto JM (2003) In: Proceedings of the AIChE 2003 spring national meeting, New Orleans, p 630
4. Zhou Z, Cheng Z, Cao Y, Zhang J, Yang D, Yuan W (2007) Chem Eng Technol 30:105
5. Gaspar AB, dos Santos GR, de Souza Costa R, da Silva MAP (2008) Catal Today 133:400
6. Debuisschert Q, Conso I, Fritz A (2003) Commercial applications of pyrolysis gasoline upgrading. In: 2nd Russian petrochemical technology conference, Moscow
7. Badano J, Lederhos C, Quiroga M, L'Argentière P, Coloma-Pascual F (2010) Quim Nova 33:48
8. Boudart M, Hwang HS (1975) J Catal 39:44
9. Paryjczac T, Szymura JA, Anorg Z (1979) Allg Chem 449:105
10. Wang CB, Lin H-K, Ho C-M (2002) J Mol Catal A Chem 180:285
11. Scholten JJF, Pijpers AP, Hustings AML (1985) Catal Rev Sci Eng 27:151
12. Matyi RJ, Schwartz LH, Butt JB (1987) Catal Rev Sci Eng 29:41
13. Lederhos CR, L'Argentière PC, Coloma-Pascual F, Fígoli NS (2006) Catal Lett 110:23
14. Hughes R (1984) In: Javanovich HB (ed) Desactivation of catalysts, chapter 2. Academic Press, London
15. Hwang CP, Yeh CT, Zhu Q (1999) Catal Today 51:93
16. Liu Y, Huang F-Y, Li J-M, Weng W-Z, Luo C-R, Wang M-L, Xia W-S, Huang C-J, Wan H-L (2008) J Catal 256:192
17. Reddy PSS, Babu NS, Pasha N, Lingaiah N, Prasad PSS (2008) Catal Commun 9:2303
18. Naito S, Tanaka H, Kado S, Miyao T, Naito S, Okumura K, Kunimori K, Tomishige K (2008) J Catal 259:138
19. Lieske H, Liets G, Spindler H, Völter J (1983) J Catal 81:8
20. Völter J (1986) In: Červený L (ed) Studies in surface science and catalysis, vol 27, chapter 10. Elsevier Science Publishers B.V., Amsterdam
21. Reyes P, Pecchi G, Morales M, Fierro JLG (1997) Appl Catal A Gen 163:145
22. Navarro RM, Pawelwc B, Trejo JM, Mariscal R, Fierro JLG (2000) J Catal 189:184
23. Tonetto GM, Damiani DE (2003) J Mol Catal A Chem 202:289
24. Ferrer V, Moronta A, Sánchez J, Solano R, Bernal S, Finol D (2005) Catal Today 107:487
25. Cheikhi N, Kacimi M, Rouimi M, Ziyad M, Liotta LF, Pantaleo G, Deganello G (2005) J Catal 232:257
26. Alegre VV, da Silva MAP, Schmal M (2006) Catal Commun 7:314
27. Noronha FB, Aranda DAG, Ordine AP, Schmal M (2000) Catal Today 57:275
28. Pinna F, Menegazzo F, Signoretto M, Canton P, Fagherazzi G, Pernicone N (2001) Appl Catal A Gen 219:195
29. Sales EA, Jove J, de Jesus Mendez M, Bozon-Verduraz F (2000) J Catal 195:88
30. Hu S-C, Chen Y-W (2001) Ind Eng Chem Res 40:6099
31. Hadjiivanov K, Lavalley J-C, Lamotte J, Maugé F, Saint-Just J, Che M (1998) J Catal 176:415
32. Simone DO, Kennelly T, Brungard NL, Farrauto RJ (1991) Appl Catal 70:87
33. Gaspar AB, Dieguez LC (2000) Appl Catal A Gen 201:241
34. Gaspar AB, Dieguez LC (2003) J Catal 220:309
35. Mazzieri V, Coloma-Pascual F, Arcoya A, L'Argentière PC, Fígoli NS (2003) Appl Surf Sci 210:222
36. Okal J, Zawadzki M, Kępiński L, Krajczyk L, Tylus W (2007) Appl Catal A Gen 319:202
37. NIST (2007) X-ray photoelectron spectroscopy database NIST standard reference database 20, version 3.5 (web version). National Institute of Standards and Technology, USA
38. Bozon-Verduraz F, Omar A, Escard J, Pontvianne B (1987) J Catal 55:126
39. Fígoli NS, L'Argentière PC, Arcoya A, Seoane XL (1995) J Catal 155:95
40. Arcoya A, Seoane XL, Gómez-Sainero LM (2003) Appl Surf Sci 211:341
41. L'Argentère PC, Cañón MG, Fígoli NS (1995) Appl Surf Sci 89:63
42. Kiskinova MP (1982) In: Delmon B, Yates JT (eds) Studies in surface science and catalysis, vol 70, chapter 5. Elsevier Science Publishers B.V., Amsterdam
43. Shriver DF, Atkins PW, Langford CH (1994) Inorganic chemistry, 3rd edn. WH Freeman and Co., New York, p 258